An Affine Invariant of Parallelograms and Its Application to Camera Calibration and 3D Reconstruction

F.C. Wu, F.Q. Duan, and Z.Y. Hu

National Laboratory of Pattern Recognition,
Institute of Automation, Chinese Academy of Sciences,
P.O. Box 2728, Beijing 100080, P.R. China
{fcwu, fqduan, huzy}@nlpr.ia.ac.cn

Abstract. In this work, a new affine invariant of parallelograms is introduced, and the explicit constraint equations between the intrinsic matrix of a camera and the similar invariants of a parallelogram or a parallelepiped are established using this affine invariant. Camera calibration and 3D reconstruction from parallelograms are systematically studied based on these constraints. The proposed theoretical results and algorithms have wide applicability as parallelograms and parallelepipeds are not rare in man-made scenes. Experimental results on synthetic and real images validate the proposed approaches.

1 Introduction

Camera calibration is a necessary step to extract metric information from 2D images. The camera calibration can be classified as: (1). Calibrated object based approaches, such as calibration based on 3D object [1], [2], [3], 2D planar object [4], [5], and 1D line segment [6]. (2). Self-calibration, such as calibration based on Kurppa's equations [7], [8], [9], the absolute conic and the absolute quadric [10], [11], [12], [13]. (3). Scene's structure information or camera's motion information based calibration, such as calibration based on parallelism [14], [16], orthogonality [15], [16], and pure rotation of camera [17]. In the paper, our attention is focused on parallelism based camera calibration.

We find a new affine invariant of parallelograms, which is one of our main contributions in the paper. Although the affine invariant is very simple in mathematics, the projections of parallelograms and parallelepipeds, as well as the explicit constraint equations between the intrinsic matrix of a camera and the similar invariants of a parallelogram or parallelepiped are easily obtained by this affine invariant. Based on these results, we can obtain the following conclusions: From the projections of a parallelogram across n views, 2(n-1) quadratic constraint equations on the camera intrinsic parameters can be obtained. In particular, from the projections of a rectangle or diamond across n views, n linear constraint equations and (n-1) quadratic constraint equations are obtained; From the projections of m coplanar parallelograms across n views, there exist at most 2n independent quadratic constraints on the intrinsic parameters of

A. Leonardis, H. Bischof, and A. Pinz (Eds.): ECCV 2006, Part II, LNCS 3952, pp. 191–204, 2006.
© Springer-Verlag Berlin Heidelberg 2006

cameras. In particular, if there are two parallelograms with the same similar parameters or with the same side-lengths in the scene, then 2n linear constraints can be obtained; From the projections of m non-coplanar parallelograms across n views, the intrinsic parameters and the motion parameters of cameras, the similar invariants of parallelograms, and the global Euclidean reconstruction of parallelograms can be linearly computed using some prior knowledge on the cameras or on the parallelograms.

For camera calibration based on a single parallelogram, to our best knowledge, the quadratic constraint equations obtained in the paper seem to be original, and do not appear in other places. For rectangle and diamond, the usually used constraints in the literature are the linear constrains, which come from orthogonality, the quadratic constraints given in the paper are of new discovery. For non-coplanar parallelograms based camera calibration and Euclidean reconstruction, our calibration method is similar to the classical self-calibration, only difference is that in our method, the use of the prior knowledge of the parallelograms makes the number of required images decrease.

M. Wilczkowiak, P. Sturm and E. Boyer reported their works on parallelepipeds in [16]. They use the factorization-based approach to compute the intrinsic parameters and the motion parameters of cameras, the similar invariants of parallelepipeds, and the global Euclidean reconstruction of parallelepipeds. In our work, the case of parallelepipeds can be integrated into the parallelogram-based framework as a special case of multiple non-coplanar parallelograms. As the factorization-based approach, our method can also compute camera motion parameters and Euclidean reconstruction of the parallelepipeds simultaneously.

In the paper, a 3D point is denoted by $\mathbf{X} = [\mathrm{x},\ \mathrm{y},\ \mathrm{z}]^\tau$, and a 2D point is denoted by $\mathbf{m} = [\mathrm{u},\ \mathrm{v},\ 1]^\tau$. The camera is of the pinhole model, then under the camera coordinate system, a 3D point $\mathbf{X}$ is projected to its image point $\mathbf{m}$ by $\alpha\mathbf{m} = \mathrm{K}\mathbf{X}$, where α is the projection depth of 3D point $\mathbf{X}$, K the camera intrinsic matrix.

The paper is organized as follows. In Section 2, the invariants of parallelograms are introduced, and the projections of parallelograms or parallelepipeds, as well as the explicit constraint equations between the intrinsic matrix of a camera and the similar invariants of a parallelogram or a parallelepiped are shown. Camera calibration and 3D reconstruction are elaborated in Section 3. Experiments are reported in Section 4. Conclusions are given at the end of this paper.

2 Invariants and Projections of Parallelograms

2.1 Invariants of Parallelograms

Let $\{\mathbf{X}_i : i = 1, 2, 3, 4\}$ be the four vertices of a parallelogram, and we always assume $\overrightarrow{\mathbf{X}_1\mathbf{X}_2} = \overrightarrow{\mathbf{X}_3\mathbf{X}_4}$ in the paper. Then, the parameters,

$$\mathrm{t} = \frac{||\mathbf{X}_3 - \mathbf{X}_1||}{||\mathbf{X}_2 - \mathbf{X}_1||}, \quad \cos\theta = \frac{(\mathbf{X}_3 - \mathbf{X}_1)^\tau(\mathbf{X}_2 - \mathbf{X}_1)}{||\mathbf{X}_3 - \mathbf{X}_1|| \cdot ||\mathbf{X}_2 - \mathbf{X}_1||}, \tag{1}$$

are the similar invariants since similarity transformation preserves the length ratio of two line segments and the angle of two lines. The parameters $\{\mathrm{t}, \theta\}$ in fact determine the shape of a parallelogram.

Definition 2.1. *Given a parallelogram* $\{\mathbf{X}_i : i = 1, 2, 3, 4\}$*, the matrix:*

$$\eta = \begin{bmatrix} 1 & \mathrm{t}\cos\theta \\ \mathrm{t}\cos\theta & \mathrm{t}^2 \end{bmatrix} \tag{2}$$

is called the similar parameter matrix of this parallelogram.

Next, we introduce an affine invariant of parallelograms, which is crucial in the paper. From $\overrightarrow{\mathbf{X}_1\mathbf{X}_2} = \overrightarrow{\mathbf{X}_3\mathbf{X}_4}$, we have $\mathbf{X}_4 - \mathbf{X}_3 = \mathbf{X}_2 - \mathbf{X}_1$, and thus,

$$\mathbf{X}_4 = \mathbf{X}_2 - \mathbf{X}_1 + \mathbf{X}_3 \ = [\mathbf{X}_1, \mathbf{X}_2, \mathbf{X}_3][-1, 1, 1]^\tau.$$

Let $\mathrm{X} = [\mathbf{X}_1, \mathbf{X}_2, \mathbf{X}_3]$, then

$$\mathrm{X}^{-1}\mathbf{X}_4 = [-1, 1, 1]^\tau. \tag{3}$$

Because an affine transformation preserves the parallelism and the length ratio of two parallel segments, the equation (3) is an affine invariant of parallelograms.

2.2 Projections of Parallelograms

From the affine invariant (3), we can easily obtain the projection of parallelograms and the explicit constraint equations between the camera intrinsic parameters and the similar invariants of a parallelogram.

Proposition 2.1. *Suppose* $\{\mathbf{m}_i\}$ *are image of a parallelogram* $\{\mathbf{X}_i\}$*, and let*

$$[\mathrm{q}_1, \mathrm{q}_2, \mathrm{q}_3]^\tau = [-\mathbf{m}_1, \mathbf{m}_2, \mathbf{m}_3]^{-1}\mathbf{m}_4, \mathrm{L} = [\mathrm{q}_2\mathbf{m}_2 - \mathrm{q}_1\mathbf{m}_1, \mathrm{q}_3\mathbf{m}_3 - \mathrm{q}_1\mathbf{m}_1]. \tag{4}$$

Then we have:

1. Under the camera coordinate system,

$$\mathbf{X}_i = \alpha_4 \mathrm{q}_i \mathrm{K}^{-1}\mathbf{m}_i, i = 1, 2, 3, 4^1 \tag{5}$$

2. The intrinsic parameters of the camera and the similar invariants of the parallelogram satisfy:

$$(||\mathbf{X}_2 - \mathbf{X}_1||^2/\alpha_4^2)\eta = \mathrm{L}^\tau \varpi \mathrm{L}. \tag{6}$$

Where α_4 *is the projection depth of point* $\mathbf{X}_4$; $\quad \varpi = \mathrm{K}^{-\tau}\mathrm{K}^{-1}$ *is IAC .*

Proof. Under the camera coordinate system, we have

$$\mathbf{X}_i = \alpha_i \mathrm{K}^{-1}\mathbf{m}_i, \ i = 1, 2, 3, 4. \tag{7}$$

[1] In the paper, we always assume $\mathrm{q}_4 = 1$.

Thus, $\mathrm{X} = [\mathbf{X}_1, \mathbf{X}_2, \mathbf{X}_3] = \mathrm{K}^{-1}[\mathbf{m}_1, \mathbf{m}_2, \mathbf{m}_3] diag[\alpha_1, \alpha_2, \alpha_3]$. Hence, we obtain $\mathrm{X}^{-1} = diag[1/\alpha_1, 1/\alpha_2, 1/\alpha_3][\mathbf{m}_1, \mathbf{m}_2, \mathbf{m}_3]^{-1}\mathrm{K}$, and

$$\begin{aligned} \mathrm{X}^{-1}\mathbf{X}_4 &= diag[1/\alpha_1, 1/\alpha_2, 1/\alpha_3][\mathbf{m}_1, \mathbf{m}_2, \mathbf{m}_3]^{-1}\mathrm{K}(\alpha_4\mathrm{K}^{-1}\mathbf{m}_4) \\ &= diag[\alpha_4/\alpha_1, \alpha_4/\alpha_2, \alpha_4/\alpha_3][\mathbf{m}_1, \mathbf{m}_2, \mathbf{m}_3]^{-1}\mathbf{m}_4 \\ &= [-\alpha_4\mathrm{q}_1/\alpha_1, \alpha_4\mathrm{q}_2/\alpha_2, \alpha_4\mathrm{q}_3/\alpha_3]^\tau \end{aligned} .$$

By the affine invariant (3), we have $\alpha_i = \alpha_4\mathrm{q}_i, i = 1, 2, 3$. Substituting them into the equation (7), we obtain the equation (5).

We have $\mathbf{X}_j - \mathbf{X}_1 = \alpha_4\mathrm{K}^{-1}(\mathrm{q}_j\mathbf{m}_j - \mathrm{q}_1\mathbf{m}_1)$ by the equation (5), and thus,

$$||\mathbf{X}_2 - \mathbf{X}_1||^2\eta = \begin{bmatrix} (\mathbf{X}_2 - \mathbf{X}_1)^\tau(\mathbf{X}_2 - \mathbf{X}_1) & (\mathbf{X}_2 - \mathbf{X}_1)^\tau(\mathbf{X}_3 - \mathbf{X}_1) \\ (\mathbf{X}_2 - \mathbf{X}_1)^\tau(\mathbf{X}_3 - \mathbf{X}_1) & (\mathbf{X}_3 - \mathbf{X}_1)^\tau(\mathbf{X}_3 - \mathbf{X}_1) \end{bmatrix} = \alpha_4^2\mathrm{L}^\tau\varpi\mathrm{L}.$$

Hence, the equation (6) holds.

Remark 2.1. Since $\mathbf{X}_4 - \mathbf{X}_3 = \mathbf{X}_2 - \mathbf{X}_1$ and $\mathbf{X}_4 - \mathbf{X}_2 = \mathbf{X}_3 - \mathbf{X}_1$, from the equations (5), we can obtain $\mathrm{q}_2\mathbf{m}_2 - \mathrm{q}_1\mathbf{m}_1 = \mathrm{q}_4\mathbf{m}_4 - \mathrm{q}_3\mathbf{m}_3 \stackrel{\Delta}{=} \mathbf{v}_1$, $\mathrm{q}_3\mathbf{m}_3 - \mathrm{q}_1\mathbf{m}_1 = \mathrm{q}_4\mathbf{m}_4 - \mathrm{q}_2\mathbf{m}_2 \stackrel{\Delta}{=} \mathbf{v}_2$. It is not difficult to see that $\mathbf{v}_1(\mathbf{v}_2)$ is a homogeneous coordinate of the vanishing point of the parallel sides $\mathbf{X}_1\mathbf{X}_2 // \mathbf{X}_3\mathbf{X}_4$ ($\mathbf{X}_1\mathbf{X}_3 // \mathbf{X}_2\mathbf{X}_4$). This is because $\mathbf{v}_1^\tau(\mathbf{m}_1 \times \mathbf{m}_2) = \mathbf{v}_1^\tau(\mathbf{m}_3 \times \mathbf{m}_4) = 0$, $\mathbf{v}_2^\tau(\mathbf{m}_1 \times \mathbf{m}_3) = \mathbf{v}_2^\tau(\mathbf{m}_2 \times \mathbf{m}_4) = 0$.

If the camera intrinsic parameters are known, we have following corollaries:

Corollary 2.1. *From the image of a parallelogram, we can recover its shape, i.e., we can determine its similar invariants.*

Corollary 2.2. *If the length of one side of a parallelogram is known, from its image we can determine the length of the other side and the distances from the parallelogram vertices to the camera center.*

Remark 2.2. In the classical PnP problem [18], in order to compute the distances between control points and the camera center from images of the control points, it is necessary to know the distances between each pair of control points. From the corollary 2.1 and 2.2, we can obtain an interesting result: If the four control points are vertices of a parallelogram, we only need to know the distance between a pair of control points for computing the distances between these control points and the camera center.

2.3 Projections of Parallelepipeds

Let $\{\mathbf{X}_1, ..., \mathbf{X}_8\}$ be 8 vertices of a parallelepiped, and we always assume $\overrightarrow{\mathbf{X}_1\mathbf{X}_2} = \overrightarrow{\mathbf{X}_3\mathbf{X}_4} = \overrightarrow{\mathbf{X}_5\mathbf{X}_6} = \overrightarrow{\mathbf{X}_7\mathbf{X}_8}$. Then, the parameters

$$\mathrm{t}_1 = \frac{||\mathbf{X}_3 - \mathbf{X}_1||}{||\mathbf{X}_2 - \mathbf{X}_1||}, \quad \mathrm{t}_2 = \frac{||\mathbf{X}_5 - \mathbf{X}_1||}{||\mathbf{X}_2 - \mathbf{X}_1||}, \quad \cos\theta = \frac{(\mathbf{X}_3 - \mathbf{X}_1)^\tau(\mathbf{X}_2 - \mathbf{X}_1)}{||\mathbf{X}_3 - \mathbf{X}_1|| \cdot ||\mathbf{X}_2 - \mathbf{X}_1||},$$

$$\cos\phi = \frac{(\mathbf{X}_5 - \mathbf{X}_1)^\tau(\mathbf{X}_2 - \mathbf{X}_1)}{||\mathbf{X}_5 - \mathbf{X}_1|| \cdot ||\mathbf{X}_2 - \mathbf{X}_1||}, \quad \cos\varphi = \frac{(\mathbf{X}_5 - \mathbf{X}_1)^\tau(\mathbf{X}_3 - \mathbf{X}_1)}{||\mathbf{X}_5 - \mathbf{X}_1|| \cdot ||\mathbf{X}_3 - \mathbf{X}_1||},$$

are the similar invariants of parallelepipeds, and they determine the shape of a parallelepiped.

Definition 2.2. *Given a parallelepiped*$\{\mathbf{X}_i\}$*, the matrix:*

$$\mu = \begin{bmatrix} 1 & \mathrm{t}_1\cos\theta & \mathrm{t}_2\cos\phi \\ \mathrm{t}_1\cos\theta & \mathrm{t}_1^2 & \mathrm{t}_1\mathrm{t}_2\cos\varphi \\ \mathrm{t}_2\cos\phi & \mathrm{t}_1\mathrm{t}_2\cos\varphi & \mathrm{t}_2^2 \end{bmatrix} \tag{8}$$

is called the similar parameter matrix of this parallelepiped.

Suppose $\{\mathbf{m}_i\}$ are the image of parallelepiped $\{\mathbf{X}_i\}$, and let

$$[\mathrm{q}_1,\ \mathrm{q}_2,\ \mathrm{q}_3]^\tau = [-\mathbf{m}_1,\ \mathbf{m}_2,\ \mathbf{m}_3]^{-1}\mathbf{m}_4,\ [\mathrm{q}_5,\ \mathrm{q}_6,\ \tilde{\mathrm{q}}_3]^\tau = [-\mathbf{m}_5,\ \mathbf{m}_6,\ \mathbf{m}_3]^{-1}\mathbf{m}_4.$$

By proposition 2.1, we have $\alpha_4\mathrm{q}_3\mathrm{K}^{-1}\mathbf{m}_3 = \mathbf{X}_3 = \alpha_4\tilde{\mathrm{q}}_3\mathrm{K}^{-1}\mathbf{m}_3$, and thus, $\mathrm{q}_3 = \tilde{\mathrm{q}}_3$. Hence,

$$[\mathrm{q}_1,\ \mathrm{q}_2,\ \mathrm{q}_3, \mathrm{q}_5, \mathrm{q}_6]^\tau = (\mathrm{A}^\tau\mathrm{A})^{-1}\mathrm{A}^\tau \begin{bmatrix} \mathbf{m}_4 \\ \mathbf{m}_4 \end{bmatrix}, \tag{9}$$

where $\mathrm{A} = \begin{bmatrix} -\mathbf{m}_1 & \mathbf{m}_2 & \mathbf{m}_3 & \mathbf{0} & \mathbf{0} \\ \mathbf{0} & \mathbf{0} & \mathbf{m}_3 & -\mathbf{m}_5 & \mathbf{m}_6 \end{bmatrix}$. We can prove the following proposition.

Proposition 2.2. *Let* $\mathrm{M} = [\mathrm{q}_2\mathbf{m}_2 - \mathrm{q}_1\mathbf{m}_1,\ \mathrm{q}_3\mathbf{m}_3 - \mathrm{q}_1\mathbf{m}_1, \mathrm{q}_5\mathbf{m}_5 - \mathrm{q}_1\mathbf{m}_1]$*. Then, we have:*

1. The coordinates of vertex $\mathbf{X}_i$ *under the camera coordinate system can be expressed as*:

$$\mathbf{X}_i = \alpha_4\mathrm{q}_i\mathrm{K}^{-1}\mathbf{m}_i, i = 1, 2...6. \tag{10}$$

2. The intrinsic parameters of the camera and the similar invariants of the parallelepiped satisfy:

$$(||\mathbf{X}_2 - \mathbf{X}_1||^2/\alpha_4^2)\mu = \mathrm{M}^\tau\varpi\mathrm{M}. \tag{11}$$

Remark 2.3. The matrix M can be computed directly from the image of a parallelepiped, which does not depend on the similar invariants. The equation (11) establishes a duality between the intrinsic parameters of a camera and the similar invariants of a parallelepiped. The result is also obtained in [16] using a different method, but they do not show the explicit expression of matrix M.

3 Calibration and 3D Reconstruction

In this section, we only discuss the camera calibration and 3D reconstruction based on parallelograms. The parallelepipeds based calibration and 3D reconstruction are similar to those on non-coplanar parallelograms. Here we omit the calibration and 3D reconstruction based on parallelepipeds due to space limit.

3.1 m Coplanar Parallelograms in n Views

Proposition 3.1. *Given the n images*$\{\mathbf{m}_{ki}^{(j)} : i = 1, 2, 3, 4; j = 1, 2...n\}$ *of m coplanar parallelograms* $\{\mathbf{X}_{ki}\}$, k=1, 2... m, *let*

$$[\mathrm{q}_{k1}^{(j)}, \mathrm{q}_{k2}^{(j)}, \mathrm{q}_{k3}^{(j)}]^{\tau} = [-\mathbf{m}_{k1}^{(j)}, \mathbf{m}_{k2}^{(j)}, \mathbf{m}_{k3}^{(j)}]^{-1}\mathbf{m}_{k4}^{(j)},$$

$$\mathrm{L}_{kj} = [\mathrm{q}_{k2}^{(j)}\mathbf{m}_{k2}^{(j)} - \mathrm{q}_{k1}^{(j)}\mathbf{m}_{k1}^{(j)}, \mathrm{q}_{k3}^{(j)}\mathbf{m}_{k3}^{(j)} - \mathrm{q}_{k1}^{(j)}\mathbf{m}_{k1}^{(j)}].$$

Then, we have 2m(n-1) quadratic constraint equations on the cameras' intrinsic parameters:

$$\frac{(\mathrm{L}_{kj}^{\tau}\varpi_j\mathrm{L}_{kj})_{11}}{(\mathrm{L}_{kj}^{\tau}\varpi_j\mathrm{L}_{kj})_{22}} = \frac{(\mathrm{L}_{k1}^{\tau}\varpi_1\mathrm{L}_{k1})_{11}}{(\mathrm{L}_{k1}^{\tau}\varpi_1\mathrm{L}_{k1})_{22}}, \quad \frac{(\mathrm{L}_{kj}^{\tau}\varpi_j\mathrm{L}_{kj})_{12}}{(\mathrm{L}_{kj}^{\tau}\varpi_j\mathrm{L}_{kj})_{22}} = \frac{(\mathrm{L}_{k1}^{\tau}\varpi_1\mathrm{L}_{k1})_{12}}{(\mathrm{L}_{k1}^{\tau}\varpi_1\mathrm{L}_{k1})_{22}}. \tag{12}$$

Where $\varpi_j = \mathbf{K}_j^{-\tau}\mathbf{K}_j^{-1}$ *is the* j^{th} *camera's IAC.*

Proof. By proposition 2.1, we have

$$||\mathbf{X}_{k2}^{(j)} - \mathbf{X}_{k1}^{(j)}||^2\eta_k = \alpha_{k4}^{(j)}\mathrm{L}_{kj}^{\tau}\varpi_j\mathrm{L}_{kj},\ j = 1, 2...n; k = 1, 2...m, \tag{13}$$

where

$$\mathbf{X}_{ki}^{(j)} = \alpha_{k4}^{(j)}\mathrm{q}_{ki}^{(j)}\mathrm{K}_j^{-1}\mathbf{m}_{ki}^{(j)},\ i = 1, 2, 3, 4 \tag{14}$$

are the coordinates of the k^{th} parallelogram's vertices under the j^{th} camera coordinate system. From $||\mathbf{X}_{k2}^{(j)} - \mathbf{X}_{k1}^{(j)}|| = ||\mathbf{X}_{k2} - \mathbf{X}_{k1}||$, $j = 1, 2...n$,we have

$$\alpha_{k4}^{(j)}\mathrm{L}_{kj}^{\tau}\varpi_j\ \mathrm{L}_{kj} = \alpha_{k4}^{(1)}\mathrm{L}_{k1}^{\tau}\varpi_1\mathrm{L}_{k1},\ j = 2, 3...n; k = 1, 2...m.$$

By eliminating the scale factors in the above equations, we can obtain 2m(n-1) quadratic constraint equations (12).

Among the 2m(n-1) quadratic constraint equations, there exist at most 2n independent constraints. Because the n images of a metric plane (i.e., the projections of circular points on the plane can be computed) can only provide 2n independent constraints for the IACs, ϖ_j, the number of independent constraints cannot exceed 2n in the case of m coplanar parallelograms.

Corollary 3.1. *If* $\{\mathbf{X}_{ki}\}$ *is a rectangle, the 2nd constraint equations in (12) become n linear constraint equations:*

$$(\mathrm{L}_{kj}^{\tau}\varpi_j\ \mathrm{L}_{kj})_{12} = 0,\ j = 1, 2...n \tag{15}$$

which are from the orthogonality.

Corollary 3.2. *If* $\{\mathbf{X}_{ki}\}$ *is a diamond, the 1st constraint equations in (12) become n linear constraint equations:*

$$(\mathrm{L}_{kj}^{\tau}\varpi_j\ \mathrm{L}_{kj})_{11} = (\mathrm{L}_{kj}^{\tau}\varpi_j\ \mathrm{L}_{kj})_{22},\ j = 1, 2...n \tag{16}$$

which are from the diamond's similar invariant, $\mathrm{t}_k = 1$.

Remark 3.1. By the orthogonality of diamond's two diagonals, we also can obtain a linear constraint equation from each image. However, we can prove that

such linear constraint equations are equivalent to the equations (16). For rectangle and diamond, the usually used constraints in the literature are the linear constrains. To our knowledge, the quadratic constraints are of new discovery.

For coplanar parallelograms, the following propositions are interesting.

Proposition 3.2. *If two parallelograms have the same similar invariants, then from their n images we can obtain 2n linear constraint equations on the intrinsic parameters of the cameras:*

$$\tilde{\mathrm{L}}_{2j}^{\tau}\varpi_j\tilde{\mathrm{L}}_{2j} = s\tilde{\mathrm{L}}_{1j}^{\tau}\varpi_j\tilde{\mathrm{L}}_{1j},\ j = 1, 2...n, \tag{17}$$

where,

$$\tilde{\mathrm{L}}_{kj} = [\tilde{\mathrm{q}}_{k2}^{(j)}\mathbf{m}_{k2}^{(j)} - \tilde{\mathrm{q}}_{k1}^{(j)}\mathbf{m}_{k1}^{(j)}, \tilde{\mathrm{q}}_{k3}^{(j)}\mathbf{m}_{k3}^{(j)} - \tilde{\mathrm{q}}_{k1}^{(j)}\mathbf{m}_{k1}^{(j)}], \tag{18}$$

$$\tilde{\mathrm{q}}_{ki}^{j} = \frac{\det[\mathrm{q}_{11}^{(j)}\mathbf{m}_{11}^{(j)}, \mathrm{q}_{12}^{(j)}\mathbf{m}_{12}^{(j)}, \mathrm{q}_{13}^{(j)}\mathbf{m}_{13}^{(j)}]}{\det[\mathrm{q}_{k1}^{(j)}\mathbf{m}_{k1}^{(j)}, \mathrm{q}_{12}^{(j)}\mathbf{m}_{12}^{(j)} - \mathrm{q}_{11}^{(j)}\mathbf{m}_{11}^{(j)}, \mathrm{q}_{13}^{(j)}\mathbf{m}_{13}^{(j)} - \mathrm{q}_{11}^{(j)}\mathbf{m}_{11}^{(j)}]}\mathrm{q}_{ki}^{j}, \tag{19}$$

$$\mathrm{s} = \frac{||(\tilde{\mathrm{q}}_{23}^{(j)}\mathbf{m}_{23}^{(j)} - \tilde{\mathrm{q}}_{21}^{(j)}\mathbf{m}_{21}^{(j)}) \times (\tilde{\mathrm{q}}_{22}^{(j)}\mathbf{m}_{22}^{(j)} - \tilde{\mathrm{q}}_{21}^{(j)}\mathbf{m}_{21}^{(j)})||}{||(\tilde{\mathrm{q}}_{13}^{(j)}\mathbf{m}_{13}^{(j)} - \tilde{\mathrm{q}}_{11}^{(j)}\mathbf{m}_{11}^{(j)}) \times (\tilde{\mathrm{q}}_{12}^{(j)}\mathbf{m}_{12}^{(j)} - \tilde{\mathrm{q}}_{11}^{(j)}\mathbf{m}_{11}^{(j)})||}. \tag{20}$$

Remark 3.2. In the above proposition, there should exist a 2D rotation between the two similar parallelograms. Otherwise, the proposition does not hold. In addition, this proposition can be generalized to the case of two similar figures with four point correspondences, i.e., if two coplanar figures with four point correspondences are similar, then from their n images we can obtain 2n linear constraint equations on the intrinsic parameters of the cameras.

Proposition 3.3. *If two parallelograms have the same side-lengths, then from their n images we can obtain 2n linear constraint equations on the intrinsic parameters of the cameras:*

$$(\tilde{\mathrm{L}}_{2j}^{\tau}\varpi_j\tilde{\mathrm{L}}_{2j})_{11} = (\tilde{\mathrm{L}}_{1j}^{\tau}\varpi_j\tilde{\mathrm{L}}_{1j})_{11},\ \ (\tilde{\mathrm{L}}_{2j}^{\tau}\varpi_j\tilde{\mathrm{L}}_{2j})_{22} = (\tilde{\mathrm{L}}_{1j}^{\tau}\varpi_j\tilde{\mathrm{L}}_{1j})_{22},\ j = 1, ...n. \tag{21}$$

3.2 m Non-coplanar Parallelograms in n Views

In this section, we mainly show a linear method in the case of multiple non-coplanar parallelograms in multiple views to compute the intrinsic parameters and the motion parameters of cameras, the similar parameters of parallelograms, and global Euclidean reconstruction of parallelograms using some prior knowledge on the cameras or on the parallelograms.

Suppose there are m parallelograms $\{\mathbf{X}_{ki}\}$,k=1, 2... m, in a scene, and among them there exist at least two non-coplanar parallelograms. Given the n images $\{\mathbf{m}_{ki}^{(j)}\}$ of the parallelograms, and let

$$[\mathrm{q}_{k1}^{(j)}, \mathrm{q}_{k2}^{(j)}, \mathrm{q}_{k3}^{(j)}]^{\tau} = [-\mathbf{m}_{k1}^{(j)}, \mathbf{m}_{k2}^{(j)}, \mathbf{m}_{k3}^{(j)}]^{-1}\mathbf{m}_{k4}^{(j)},$$

$$\mathrm{L}_{kj} = [\mathrm{q}_{k2}^{(j)}\mathbf{m}_{k2}^{(j)} - \mathrm{q}_{k1}^{(j)}\mathbf{m}_{k1}^{(j)}, \mathrm{q}_{k3}^{(j)}\mathbf{m}_{k3}^{(j)} - \mathrm{q}_{k1}^{(j)}\mathbf{m}_{k1}^{(j)}].$$

Table 1. Linear constraints on ϖ_1 from prior information of camera

Prior information of camera	Linear constraints on ϖ_1
zero skew	$(\mathrm{H}_{1j}^{-\tau}\varpi_1\mathrm{H}_{1j}^{-1})_{12}=0$
principal point at origin	$(\mathrm{H}_{1j}^{-\tau}\varpi_1\mathrm{H}_{1j}^{-1})_{13}=(\mathrm{H}_{1j}^{-\tau}\varpi_1\mathrm{H}_{1j}^{-1})_{23}=0$
known aspect ratio $\tau=\mathrm{f}_v/\mathrm{f}_u$	$\tau^2(\mathrm{H}_{1j}^{-\tau}\varpi_1\mathrm{H}_{1j}^{-1})_{22}-(\mathrm{H}_{1j}^{-\tau}\varpi_1\mathrm{H}_{1j}^{-1})_{11}=0$

Table 2. Linear constraints on ϖ_1 from prior information of parallelogram

Prior information of parallelogram	Linear constraints on ϖ_1
$\theta_k=\pi/2$	$(\mathrm{L}_{k1}^{\tau}\varpi_1\mathrm{L}_{k1})_{12}=0$
$\mathrm{t}_{k1}=1$	$(\mathrm{L}_{k1}^{\tau}\varpi_1\mathrm{L}_{k1})_{11}=(\mathrm{L}_{k1}^{\tau}\varpi_1\mathrm{L}_{k1})_{22}$
two coplanar parallelograms with the same similar invariants	constraint equations (17)
two coplanar parallelograms with the same side-lengths	constraint equations (21)

By proposition 2.1, the coordinates of the k^{th} parallelogram's vertices under the j^{th} camera coordinate system are:

$$\mathbf{X}_{ki}^{(j)}=\alpha_{k4}^{(j)}\mathrm{q}_{ki}^{(j)}\mathrm{K}_j^{-1}\mathbf{m}_{ki}^{(j)}:i=1,2,3,4. \tag{22}$$

By remark 2.1, the image points,$\mathbf{v}_{k1}^{(j)}=\mathrm{q}_{k2}^{(j)}\mathbf{m}_{k2}^{(j)}-\mathrm{q}_{k1}^{(j)}\mathbf{m}_{k1}^{(j)}$ and $\mathbf{v}_{k2}^{(j)}=\mathrm{q}_{k3}^{(j)}\mathbf{m}_{k3}^{(j)}-\mathrm{q}_{k1}^{(j)}\mathbf{m}_{k1}^{(j)}$, are the vanishing points of the two pair of parallel sides of the k^{th} parallelogram in the j^{th} image plane. We can linearly determine the infinite homography H_{1j} between the 1^{st} view and the j^{th} view from the vanishing point correspondences,$\{\mathbf{v}_{k1}^{(1)}\leftrightarrow\mathbf{v}_{k1}^{(j)},\ \mathbf{v}_{k2}^{(1)}\leftrightarrow\mathbf{v}_{k2}^{(j)},\ k=1,2...m\}$. Hence, we can obtain the 5n-5 constraint equations on the IACs:

$$\omega_j=\mathrm{s}_j\mathrm{H}_{1j}^{-\tau}\varpi_1\mathrm{H}_{1j}^{-1},j=2,3...n, \tag{23}$$

where s_j is an unknown scale factor. On the other hand, by proposition 2.2, we have the constraints on (η_k,ϖ_j):

$$\eta_k=\mathrm{t}_{kj}\mathrm{L}_{kj}^{\tau}\varpi_j\mathrm{L}_{kj},\ j=1,2...n;k=1,2...m, \tag{24}$$

where t_{kj} is an unknown scale factor.

Note that all the constraints (23) and (24) are nonlinear. However, using some prior knowledge on the cameras, from the constraints (23) we can obtain linear constrains on ϖ_1 (see Tab.1); using some prior knowledge on the parallelograms, from the constraints (24) we can also obtain linear constrains on ϖ_1 (see Tab.2).

Intrinsic parameters and similar invariants. From the above discussions, we can see that using some prior knowledge on the cameras or/and on the parallelograms, from a few images of the parallelograms we can linearly determine

ϖ_1 up to a scale factor. Once ϖ_1 is obtained, ϖ_j can be obtained up to a scale factor by the equations (23), and thus η_k can also be determined up to a scale factor by the equations (24).

After ϖ_j and η_k are determined up to scale factors, we can compute the intrinsic parameter matrix K_j from ϖ_j, e.g., using Choleskey decomposition; and setting $(\eta_k)_{11} = 1$, we obtain the similar invariants $\{\mathrm{t}_k, \theta_k\}$.

3D reconstruction and motion recovery. Let $[\mathrm{R}_j, \mathbf{t}_j]$be the motion from the 1^{st} view to the j^{th} view. By the equation (22), we have

$$\alpha_{k4}^{(j)}\mathrm{q}_{ki}^{(j)}\mathrm{K}_j^{-1}\mathbf{m}_{ki}^{(j)} = \alpha_{k4}^{(1)}\mathrm{q}_{ki}^{(1)}\mathrm{R}_j\mathrm{K}_1^{-1}\mathbf{m}_{ki}^{(1)} + \mathbf{t}_j,\ i = 1,2,3,4; k = 1,2...m, \quad (25)$$

$$\mathrm{R}_j\mathrm{K}_1^{-1}(\mathrm{q}_{ki}^{(1)}\mathbf{m}_{ki}^{(1)} - \mathrm{q}_{k1}^{(1)}\mathbf{m}_{k1}^{(1)}) = (\alpha_{k4}^{(j)}/\alpha_{k4}^{(1)})\mathrm{K}_j^{-1}(\mathrm{q}_{ki}^{(j)}\mathbf{m}_{ki}^{(j)} - \mathrm{q}_{k1}^{(j)}\mathbf{m}_{k1}^{(j)}), \quad i = 2,3,4;\ k = 1,2...m. \quad (26)$$

and thus, we can obtain $(\alpha_{k4}^{(j)}/\alpha_{k4}^{(1)})^2\mathrm{w}_{ki}^{(j)} = \mathrm{w}_{ki}^{(1)}$, where:

$$\mathrm{w}_{ki}^{(j)} = (\mathrm{q}_{ki}^{(j)}\mathbf{m}_{ki}^{(j)} - \mathrm{q}_{k1}^{(j)}\mathbf{m}_{k1}^{(j)})^\tau\varpi_j(\mathrm{q}_{ki}^{(j)}\mathbf{m}_{ki}^{(j)} - \mathrm{q}_{k1}^{(j)}\mathbf{m}_{k1}^{(j)}).$$

Then,

$$\alpha_{k4}^{(j)}/\alpha_{k4}^{(1)} = \sqrt{(1/3)\sum_{i=2}^{4}(\mathrm{w}_{ki}^{(1)}/\mathrm{w}_{ki}^{(j)})} \triangleq \beta_{kj}\ k = 1,2...m, \quad (27)$$

Substituting (27) into (26), we have

$$\mathrm{R}_j\mathrm{K}_1^{-1}(\mathrm{q}_{ki}^{(1)}\mathbf{m}_{ki}^{(1)} - \mathrm{q}_{k1}^{(1)}\mathbf{m}_{k1}^{(1)}) = \beta_{kj}\mathrm{K}_j^{-1}(\mathrm{q}_{ki}^{(j)}\mathbf{m}_{ki}^{(j)} - \mathrm{q}_{k1}^{(j)}\mathbf{m}_{k1}^{(j)}), \quad i = 2,3,4;\ k = 1,2...m. \quad (28)$$

Let

$$\mathrm{B}_{kj} = [\mathrm{q}_{k2}^{(1)}\mathbf{m}_{k2}^{(1)} - \mathrm{q}_{k1}^{(1)}\mathbf{m}_{k1}^{(1)}, \mathrm{q}_{k3}^{(1)}\mathbf{m}_{k3}^{(1)} - \mathrm{q}_{k1}^{(1)}\mathbf{m}_{k1}^{(1)}, \mathrm{q}_{k4}^{(1)}\mathbf{m}_{k4}^{(1)} - \mathrm{q}_{k1}^{(1)}\mathbf{m}_{k1}^{(1)}], \quad (29)$$

$$\mathrm{C}_{kj} = [\mathrm{q}_{k2}^{(j)}\mathbf{m}_{k2}^{(j)} - \mathrm{q}_{k1}^{(j)}\mathbf{m}_{k1}^{(j)}, \mathrm{q}_{k3}^{(j)}\mathbf{m}_{k3}^{(j)} - \mathrm{q}_{k1}^{(j)}\mathbf{m}_{k1}^{(j)}, \mathrm{q}_{k4}^{(j)}\mathbf{m}_{k4}^{(j)} - \mathrm{q}_{k1}^{(j)}\mathbf{m}_{k1}^{(j)}]. \quad (30)$$

Then, the equations (28) can be written as the matrix form:

$$\mathrm{R}_j\mathrm{K}_1^{-1}[\mathrm{B}_{1j}, \mathrm{B}_{2j}, ..., \mathrm{B}_{mj}] = \mathrm{K}_j^{-1}[\beta_{1j}\mathrm{C}_{1j}, \beta_{2j}\mathrm{C}_{2j}, ..., \beta_{mj}\mathrm{C}_{mj}].$$

Because there exist non-coplanar parallelograms, $rank[\mathrm{B}_{1j}, \mathrm{B}_{2j}, ..., \mathrm{B}_{mj}] = 3$, and thus we have

$$\mathrm{R}_j = \mathrm{K}_j^{-1}\underbrace{[\beta_{1j}\mathrm{C}_{1j}, \beta_{2j}\mathrm{C}_{2j}, ..., \beta_{mj}\mathrm{C}_{mj}][\mathrm{B}_{1j}, \mathrm{B}_{2j}, ..., \mathrm{B}_{mj}]^+}_{\mathrm{D}_j}\mathrm{K}_1. \quad (31)$$

Substituting (27) and (31) into (25), we can obtain the constraints on $(\alpha_{k4}^{(1)}, \mathbf{t}_j)$:

$$(\mathrm{q}_{ki}^{(1)}\mathrm{D}_j\mathbf{m}_{ki}^{(1)} - \beta_{kj}\mathrm{q}_{ki}^{(j)}\mathbf{m}_{ki}^{(j)})\alpha_{k4}^{(1)} + \mathrm{K}_j\mathbf{t}_j = 0. \quad (32)$$

Let

$$\mathrm{E}_{kj} = \begin{bmatrix} \mathrm{q}_{k1}^{(1)}\mathrm{D}_j\mathbf{m}_{k1}^{(1)} - \beta_{kj}\mathrm{q}_{k1}^{(j)}\mathbf{m}_{k1}^{(j)} \\ \vdots \\ \mathrm{q}_{k4}^{(1)}\mathrm{D}_j\mathbf{m}_{k4}^{(1)} - \beta_{kj}\mathrm{q}_{k4}^{(j)}\mathbf{m}_{k4}^{(j)} \end{bmatrix}, k = 1, 2...m; j = 2, 3...n, \tag{33}$$

$\mathrm{E}_j = diag[\mathrm{E}_{1j}, \mathrm{E}_{2j}, ..., \mathrm{E}_{mj}]$, $\mathrm{C} = [\underbrace{\mathrm{I}_3, \mathrm{I}_3, ..., \mathrm{I}_3}_{12m}]^\tau$ (I_3 is the unit matrix of order 3).

Then, the equations (32) can be written as the matrix form:

$$\underbrace{\begin{bmatrix} \mathrm{E}_2 & \mathrm{CK}_2 & & \\ \vdots & & \ddots & \\ \mathrm{E}_n & & & \mathrm{CK}_n \end{bmatrix}}_{E} \begin{bmatrix} \alpha \\ \tau \end{bmatrix} = 0, \tag{34}$$

where $\alpha = [\alpha_{14}^{(1)}, \alpha_{24}^{(1)}, ..., \alpha_{m4}^{(1)}]^\tau$, $\tau = [\mathbf{t}_2^\tau, \mathbf{t}_3^\tau, ..., \mathbf{t}_n^\tau]^\tau$. Hence, the least squares solution of the equations (32) is the unit right singular vector corresponding to the smallest singular value of E, and denoted as

$$\tilde{\alpha} = \left[\tilde{\alpha}_{14}^{(1)}, \tilde{\alpha}_{24}^{(1)}, ..., \tilde{\alpha}_{m4}^{(1)}\right]^\tau, \tilde{\tau} = \left[\tilde{\mathbf{t}}_2^\tau, \tilde{\mathbf{t}}_3^\tau, ..., \tilde{\mathbf{t}}_n^\tau\right]^\tau. \tag{35}$$

By the equations (22), the coordinates of the parallelograms' vertices under the 1^{st} camera coordinate system can be expression as

$$\mathbf{X}_{ki}^{(1)} = \alpha_{k4}^{(1)}\mathrm{q}_{ki}^{(1)}\mathrm{K}_1^{-1}\mathbf{m}_{ki}^{(1)}, i = 1, 2, 3, 4; k = 1, 2...m.$$

Substituting $\alpha_{k4}^{(1)} = \tilde{\alpha}_{k4}^{(1)}$ into the above equations, we can obtain an Euclidean reconstruction of the parallelograms under the 1^{st} camera coordinate system:

$$\mathbf{X}_{ki}^{(1)} = \tilde{\alpha}_{k4}^{(1)}\mathrm{q}_{ki}^{(1)}\mathrm{K}_1^{-1}\mathbf{m}_{ki}^{(1)}, i = 1, 2, 3, 4; k = 1, 2, ..., m. \tag{36}$$

4 Experimental Results

4.1 Synthetic Data

The case of parallelograms. This experiment is to study the performance of the calibration using parallelograms. We only report the calibration from one image. The used prior information on the camera was zero skew and known principal point. The camera's setting is $(f_u, f_v, s, u_0, v_0) = (1000, 900, 0, 512, 512)$. The image resolution is of 1024×1024 pixels. The parallelograms were generated as follows: At first, a parallelepiped was generated, then, we randomly generated two parallelograms with the same similar invariants on one plane and two parallelograms with the same side-lengths on the other plane. As [16], the parallelepiped orientation varies from that shown in Fig.1 left (both of the two planes are parallel to x axes of the camera) to that of Fig.1 right (a degenerate configuration, both of the two planes are parallel to the optical axes).

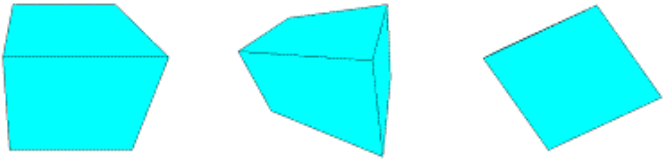

Fig. 1. Parallelepiped orientations in the case of parallelograms

The continuous rotation between the two positions is parameterized by an angle ranging from 0^o (Fig.1 left) to 90^o (Fig.1 right). In order to provide more statistically meaningful results, we performed 100 trials. In each trial, Gaussian noise of standard deviation 1 pixel was added to each vertex image of the parallelograms. Calibration was considered to be failed if the estimated matrix ω was not positive definite.

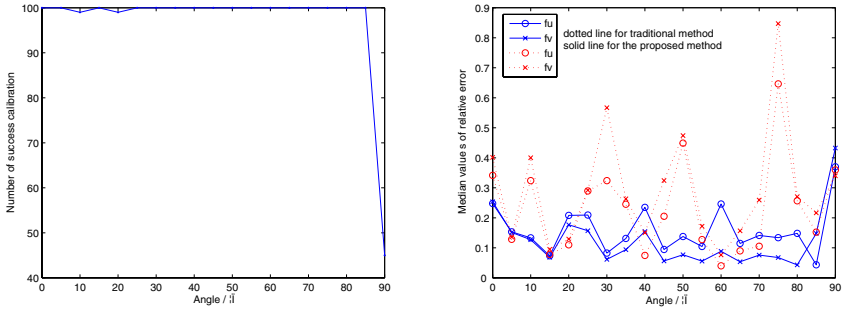

Fig. 2. Calibration results with the change of the relative camera-parallelepiped rotation angle. Left: the number of successful calibration; Right: the relative error of the estimation of f_u and f_v.

The calibration method described here is compared with the traditional method. The traditional method uses the 16 vertices of the parallelograms to estimate the projection matrix, and determines intrinsic parameter by QR-decomposition of the 3×3 sub-matrix of the projection matrix. Fig.2 shows the number of successful calibrations of the proposed method and the relative error of the estimated intrinsic parameters for both the parallelogram-based approach and the tradition approach, where the value at each pose is the mean of 100 independent trials (computed using only results of trails with valid calibration for the proposed method). It can be seen from Fig.2 that the parallelogram-based method is superior to the traditional method in general cases.

The case of parallelepipeds. This experiment is to study the performance of the calibration, camera motion estimation and reconstruction using parallelepipeds. We only report the case of one parallelepiped in two views. The two cameras' settings are $(f_u, f_v, s, u_0, v_0) = (1000, 900, 0, 512, 512)$ and

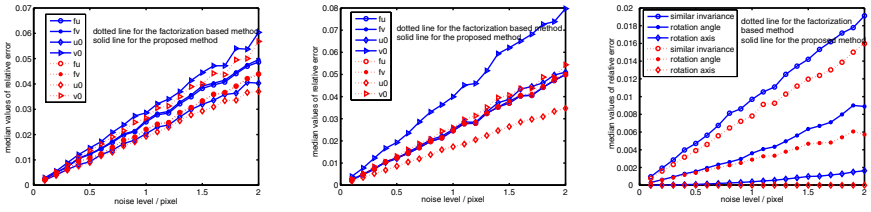

Fig. 3. Results for case of parallelepipeds (dotted line: factorization-based method, solid line: our method). left: the first camera parameters. middle: the second camera parameters. left: camera motion parameters and similar invariants.

(900, 800, 0, 512, 512) respectively. The image resolution is of 1024×1024 pixels. The test data were generated by a random rigid transformation of a canonical cube. We performed 1000 tests. In each test, Gaussian noise was added to each image point of the parallelepiped vertices. The used prior information was: the parallelepiped has three right angles and the cameras have zero skew.

Our proposed method is compared to M.Wilczkowiak's factorization-based method. Fig.3 shows the relative error of the estimated parameters for both methods, where the value at each noise level is the mean of 1000 independent tests. From the figure, we can see that the two approaches perform comparably and the factorization-based method is slightly better.

4.2 Results on Real Scenes

Calibration object. Fig.4(up)shows the original image and the calibration parallelograms. The two coplanar parallelograms are similar, and the other two coplanar parallelograms are of same side-lengths. The image size is 2048×1536. The used prior information is zero skew and known principal point. The camera parameters obtained by the traditional method and the proposed method are (3723, 3715.7, 7.9, 1003.4, 759.4) and (3720.8, 3739.9, 0, 1024, 768) respectively. The estimated parameters are used for our 3D reconstruction process for comparing the calibration results of the two methods. The similar invariants of the parallelograms estimated from the two methods are shown in Tab.3. The estimated angle of the two calibration planes is 88.99^o and 89.38^o for the traditional method and proposed method respectively. From the comparison of the estimated similar invariants and the estimated angle, we can see the result is

Table 3. The comparison of the similar invariants $(t, \cos\theta)$

parallelograms	The 1th		The 2th		The 3th		The 4th	
real value	1	0	1	0	1.491	0.447	1.491	0.447
traditional method	1.01	0.004	0.982	0.019	1.501	0.442	1.497	0.472
proposed method	1.006	0.001	0.984	0.015	1.491	0.447	1.506	0.467

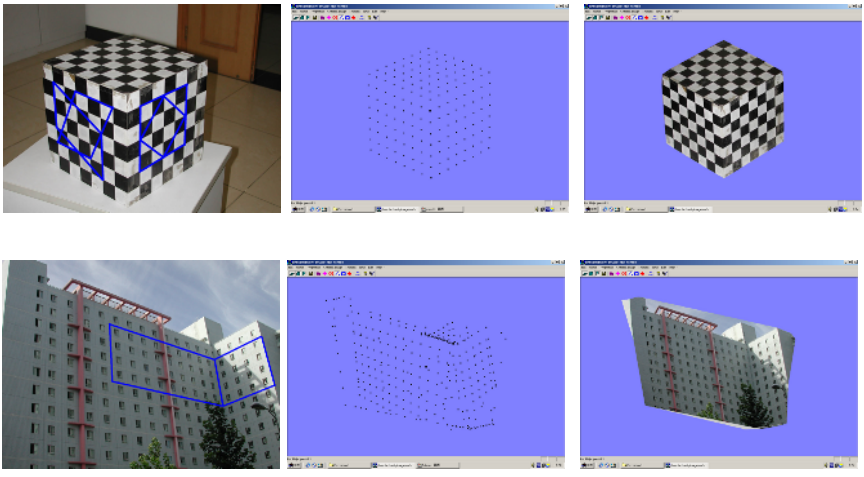

Fig. 4. Left: the original image, middle: the 3D points, right: texture mapping result from a different view

slightly better for the proposed method. Fig.4(up) shows the reconstructed 3D points by our method and the texture mapping result from a different viewpoint.

Outdoor scene. The image and the calibration parallelepiped are shown in Fig.4(low). The image size is 1024×768. The used prior information is: the parallelepiped has right angles; the camera has zero skew and unit aspect ratio. The intrinsic parameters obtained by our proposed method and by M.Wilczkowiak's method are (1354.6, 1354.6, 0, 586.3, 382) and (1359.5, 1359.5, 0, 588.5, 380) respectively. The similar invariants obtained by the two methods are $(t_1,\ t_2) = (2.6285,\ 1.1403)\quad (t_1/t_2 = 2.305)$ and $(2.6303,\ 1.1421)\quad (t_1/t_2 = 2.303)$ respectively. The real value of t_1/t_2 is 2.5. We can see the similar invariants obtained by the two methods are very close to the real value. Fig.4(low)shows the reconstructed 3D points by our method and the texture mapping result from a different viewpoint, where the estimated angle of the two calibration planes was 89.986^o. By the comparison of the similar invariants and the camera parameters, we can see the results are very close for the two approaches.

5 Conclusion

In this paper, a new affine invariant of parallelogram is introduced, by which the projections of the parallelogram and parallelepiped, and the explicit constraint equations between the camera's intrinsic matrix and the similar invariants of a parallelogram or a parallelepiped are obtained. From these constraints, we presented an approach for camera calibration, motion estimation, and 3D reconstruction from a few uncalibrated images based on some geometric constraints on the scene. Commonly available constraints, such as parallelism, coplanarity,

right angles, and length ratios, can be nicely modeled via parallelogram. The approach can deal with the scene to contain parallelograms and parallelepipeds simultaneously. Experimental results on synthetic and real images also validated the presented theoretical results and algorithms.

Acknowledgments. This study was partially supported by the National Science Foundation of China Grant No.60575019 and the National Key Basic Research and Development Program (973) Grant No. 2004CB318107.

References

1. Y.I.Abdel-Aziz, H.M.Karara: Direct linear transformation from comparator coordinates into object space coordinates. In: ASP Symposimy on Colse-Range Photogrammetry. (1971) 1–18
2. R.Tsai, R.K.Lenz: A technique for fully automous and efficient 3d robotics hand/eye calibration. IEEE Trans. Robotics and Automation **5** (1989) 345–358
3. R.Tsai: An efficient and accurate camera calibration technique for 3d machine vision. In: Proc. CVPR. (1986) 364–374
4. Zhang, Z.: Flexible camera calibration by viewing a plane from unknown orientations. In: Proc.ICCV. (1999) 666–673
5. Sturm, P., S.J.Maybank: On plane-based camera calibration: A general algorithm, singularities, applications. In: Proc. CVPR. (1999) 432–437
6. Zhang, Z.: Camera calibration with one-dimensional objects. In: Proc. ECCV. (2002) 161–174
7. J.Maybank, S., O.D.Faugeras: A theory of self-calibration of a moving camera. IJCV **8** (1992) 123–152
8. R.I.Hartley: Estimation of relative camera positions for uncalibrated cameras. In: Proc. ECCV. (1992) 579–587
9. R.I.Hartley: An algorithm for self calibration from several views. In: Proc. CVPR. (1994) 908–912
10. M.Pollefeys, Gool, L., Osterlinck, A.: The modulus constraint: a new constraint for self-calibration. In: Proc. ICPR. (1996) 31–42
11. M.Pollefeys, Gool, L.: A stratified approach to metric self-calibration. In: Proc. CVPR. (1997) 407–412
12. R.I.Hartley, Agapite, L., E.Hayman, I.Reid: Camera calibration and search for infinity. In: Proc. ICCV. (1999) 510–517
13. B.Triggs: Auto-calibration and the absolute quadric. In: Proc. CVPR. (1997) 609–614
14. B.Caprile, V.Torre: Using vanishing points for camera calibration. IJCV. **4** (1990) 127–140
15. C.Chen, C.Yu, Y.Hung: New calibration-free approach for augmented reality based on parameterized cuboid structure. In: Proc. ICCV. (1999) 30–37
16. M.Wilczkowiak, P.Sturm, Boyer, E.: Using geometric constraints through parallelepipeds for calbration and 3d modeling. IEEE-T PAMI. **27** (2005) 194–207
17. Hartely, R.: Self-calibration of stationary cameras. IJCV **22** (1997) 5–23
18. W.J.Wolfe, Mathis, D.: The perspective view of three points. IEEE-T PAMI. **13** (1991) 66–73